

Received June 10, 2020, accepted June 28, 2020, date of publication July 9, 2020, date of current version July 23, 2020.

Digital Object Identifier 10.1109/ACCESS.2020.3008289

Learning-Based IoT Data Aggregation for Disaster Scenarios

MIN PENG¹, SAHIL GARG^{ID 2}, (Member, IEEE), XIAODING WANG^{ID 1},

ABBAS BRADAI^{ID 3}, (Member, IEEE), HUI LIN^{ID 1}, AND

M. SHAMIM HOSSAIN^{ID 4,5}, (Senior Member, IEEE)

¹College of Mathematics and Informatics, Fujian Normal University, Fuzhou 350117, China

²École de technologie supérieure (ETS), Université du Québec, Montréal, QC H3C 1K3, Canada

³XLIM Research Institute, University of Poitiers, 86130 Poitiers, France

⁴Chair of Pervasive and Mobile Computing, College of Computer and Information Sciences, King Saud University, Riyadh 11543, Saudi Arabia

⁵Department of Software Engineering, College of Computer and Information Sciences, King Saud University, Riyadh 11543, Saudi Arabia

Corresponding authors: Hui Lin (linhui@fjnu.edu.cn) and Xiaoding Wang (wangdin1982@163.com)

This work was supported by the Deanship of Scientific Research, King Saud University, Riyadh, Saudi Arabia, through the Vice Deanship of Scientific Research Chairs: Chair of Pervasive and Mobile Computing.

ABSTRACT Industrial Internet of Everything (IIoE), as the deep integration of industry 6.0, the Internet of Things (IoT) and 6G mobile communication technology, pave the way for intelligent industry, enabling industrial optimization and automation. To ensure the high quality of services (QoS) in IIoE, tremendous real-time information generated by the pervasive smart things needs to be aggregated and processed quickly and reliably. However, a large-scale disaster could damage the entire communication network and cut off data aggregation such that Qos is compromised. In this paper, an Intelligent NIB based Data Aggregation Strategy, named (IDAS), is proposed for after disaster scenarios in IIoE. Specifically, IDAS first applies both iterative cubature kalman filter and radial basis function neural network to predict the data collection rates of survived infrastructures. Then, an energy efficient task distribution mechanism is design. Next, a deep reinforcement learning method is developed for the car-carrying NIB route design to perform corresponding task. Eventually, all data are aggregated toward the rescue headquarter by NIB deployment based on Fermat tree constructions. The theoretical analysis and simulations indicate that IDAS is not only energy efficient for after disaster scenarios but requires the least NIB consumption while compared with contemporary strategies.

INDEX TERMS Industrial Internet of Everything, after disaster, data aggregation, Deep Reinforcement Learning, NIB.

The fundamental goal of Industrial Internet of Everything (IIoE) is to inter-connect a variety of objects so that they can exchange data for industrial applications. That implies the connectivity is significant during data aggregation. Network-In-a-Box (NIB) [24] is a technology that provides connectivity among disconnected devices. Once the network is damaged in a disaster, NIBs are deployed for connectivity restoration. For simplicity, we call such NIB the stationary NIB (SNIB). However, it is difficult to carry SNIBs to the disaster scene. Therefore, vehicles are employed for NIB transportation [25]. Similarly, we call such NIB the Car-carrying NIB (CNIB). In fact, rescue equipments could be insufficient while dealing with a large-scale disaster. That provides a great opportunity for CNIBs to offer intermittent connections between survived infrastructures, i.e., communication towers,

The associate editor coordinating the review of this manuscript and approving it for publication was Sherali Zeadally^{ID}.

for distress calls or mayday signals aggregation. Although many previous works have been proposed in after disaster scenarios, they mainly focus on the number of SNIBs required and the energy cost of CNIBs disregarding the energy efficiency between aggregation ratio and energy cost.

In this paper, we propose an Intelligent Data Aggregation Strategy (IDAS) based on NIB deployment in the after disaster scenario for IIoE. Specifically, IDAS consists of an Iterative Cubature Kalman Filter and RBF Neural Network (ICKF-RBFNN) based data collection rate prediction, an energy efficient task distribution, a DRL based route design and a Fermat tree based connection. We give the details of our contributions as follows.

- 1) To ensure the data aggregation, IDAS first employs an iterative cubature Kalman filter to train the RBF neural network for data collection rate prediction. Then, an energy efficient task distribution mechanism is designed. Next, a Deep Reinforcement Learning (DRL)

method is developed for each energy efficient car-carrying NIB route design w.r.t the corresponding data collection task. Eventually, stationary NIB are deployed based on Fermat tree construction to reduce the NIB consumption. All data will be collected and aggregated toward the rescue headquarter through a connected network by car-carrying NIBs and stationary NIBs deployment.

- 2) The theoretical analysis and validation experiment show that the proposed IDAS has a higher aggregation ratio and a less energy cost while compared with contemporary strategies, meanwhile IDAS has the least NIB consumption.

We organize the rest of the paper as follows. Section I gives related work. Section II introduces the system model. The IDAS is elaborated in Section III. The experiments are presented in section IV. The conclusion is given in Section V.

I. STATE-OF-THE-ART

In an after-disaster scenario, a fundamental aspect is how to carry NIBs to reach the deployment spot. Some researches suggest leveraging vehicles for timeliness, i.e., deploying CNIBs. That suggests the route design for CNIBs should take the energy cost into consideration for lifetime extension. In the study of vehicle route design, Abbas and Younis [6] deploy vehicles on convex hulls of components for data aggregation and then they place RNs for connectivity restoration. Similarly, the RCR [3] is proposed to further shorten the vehicle routes by deploying RNs. CISIL [1] exploits hyperedges of hypergraph as vehicle routes w.r.t Delaunay triangulation. Energy cost equalization is accomplished by LEEF [2]. On the other hand, lots of previous works take energy cost into consideration w.r.t realistic terrains. In [4], stochastic geometry optimizes the RN count and energy cost. In [5], the connectivity is maintained and energy efficiency is achieved by efficient clustering and routing as well. In [8], ReBAT is designed to quantify terrains for minimum energy cost routes discovery. Wang *et al.* [7] focus on influences of realistic terrains and then develop the data aggregation algorithm of the least energy cost. In [14], the data collection rate is predicted utilizing RBFNN for data aggregation route design. Toyoshima *et al.* [15] propose Deep Q-Network (DQN) based vehicle simulation systems, which is called in this strategy DQNMDC in this paper for simplicity, considering three-dimensional environment for normal and uniform distributions of events. However, these works are not energy efficient, i.e., the trade-off between aggregation ratio and energy cost is not accomplished.

Plenty of works deploy SNIB for connectivity restoration as relays. In these works, the approximation ratio between the number of relays required and the optimal one is usually considered as the measurement metric, i.e., the less the better. Misra *et al.* [18], Yang *et al.* [17] and Efrat *et al.* [16] build weighted complete graphs, based on which different algorithms are developed. Wang *et al.* [19] utilize the star topology and the center of mass for connectivity restoration. In [20],

a straight skeleton based strategy is designed. Chen *et al.* [21] consider the case that there are obstacles on the deployment area and propose an algorithm for obstacle avoidance. In [22], a space network coding based algorithm is designed to discover the optimal route for relay deployment. In [23], the centroids of partitions are utilized to design a route for relay deployment. Compared with these works, the proposed IDAS require the least approximation ratio. That suggests IDAS is more suitable for data aggregation in the after disaster scenario for IIoE due to the number of SNIBs is limited.

II. SYSTEM MODEL

An IIoE network without the connectivity is considered in this paper, in which each node n_i represents a survived infrastructures, i.e., a communication tower. As the disaster can cause a large-scale damage, i.e., worker injury, factory collapse, communication interruptions etc., the rescue headquarter should restore the communication with injured workers through survived infrastructures. However, it is difficult to communicate with the rescue headquarter because survived infrastructures are overwhelmed by call attempts or their communications with outside world are completely cut off. In these cases, deploying NIBs, e.g., CNIBs and SNIBs, helps to reestablish communications.

As we analysed before, three important factors, namely the aggregation ratio, the energy cost and the number of NIBs, should be considered during the NIB deployment. Recall that the aggregation ratio relies on the travelling distance that somehow determines the energy cost. However, terrains of realistic environments are dominant for energy cost. That indicates the importance for terrain quantification.

TABLE 1. Notions.

Sym.	Desc.
G_i	The component i
N_m	CNIB count
n_i	i th node
η	Tolerable data loss rate
BUF	Buffer size
DCR	Data collection rate
p_i^c	Data collection position
\mathcal{F}	Energy factor
H	Hamilton cycle
$L(\cdot)$	Euclidean distance
\mathbb{E}	Energy cost
AR	Aggregation ratio
R	Communication radius of NIB
V	CNIB speed
κ	Constant coefficient
ν	Energy coefficient
r_c	Terrain risk
e_c	Terrain elevation
l_c	Travelling distance of CNIB over a cell

A. TERRAIN QUANTIFICATION

We apply the grid based quantification to measure terrain influences. Specifically, each cell c of the grid with the side length not less than the communication range of a CNIB is associated with an energy factor \mathcal{F} on a certain terrain as

$$\mathcal{F}_c = \int_{l_c} \int_{e_c} r_c, \quad (1)$$

where l_c , r_c and e_c represent the travelling distance, the risk and the elevation of c , respectively. Thus, the energy factor \mathcal{F}_T of route T is the sum of that of each sub-route T_i , which is given by

$$\mathcal{F}_T = \sum_{T_i \in T} \sum_{c \in T_i} \mathcal{F}_c \quad (2)$$

Accordingly, the energy cost of CNIB on route T , which is denoted as $\mathbb{E}_T^{Vehicle}$, is then given by

$$\mathbb{E}_T^{Vehicle} = \mathcal{F}_T \times v, \quad (3)$$

where $v \propto V$. Obviously, $\mathbb{E}_T^{Vehicle}$ is proportional to terrain influences. If a CNIB visits a component G_i on route T_i , then it collects data at a specific position p_i^c . Thus, the energy cost of a node $n_j \in G_i$ can be calculated as

$$\mathbb{E}_{n_j p_i^c}^{Node} = \kappa \times L_{n_j p_i^c}^2, \quad (4)$$

where κ is a power related constant and $L_{n_j p_i^c}$ denotes the length of the edge $(n_j p_i^c)$. Thus, we can deduce that p_i^c is the centroid of component G_i due to $p_i^c = \arg \min \sum_{n_j \in G_i} \mathbb{E}_{n_j p_i^c}^{Node}$ for network lifespan improvement. Then, the energy cost for data collection is given by

$$\mathbb{E}_T^{Node} = \sum_{T_i \in T} \sum_{C_i \in T_i} \sum_{n_j \in C_i} \mathbb{E}_{n_j p_i^c}^{Node}. \quad (5)$$

Thus, the overall energy cost of route T is then given by

$$\mathbb{E}_T = \mathbb{E}_T^{Vehicle} + \mathbb{E}_T^{Node}. \quad (6)$$

Note that reducing energy cost may somehow contradict to aggregation ratio improvement, i.e., a route of less energy cost might require a detour that results in a less aggregation ratio. Thus, we focus on developing an energy efficient data aggregation strategy to achieve the tradeoff between aggregation ratio and energy cost utilizing the minimum number of NIBs.

III. THE IDAS APPROACH

A. ICKF-RBFNN BASED DCR PREDICTION

We employ RBFNN to predict Dcr_{n_i} based on environmental data, i.e., temperature t , humidity h and pressure p . Thus, we let the number n of historical data (t_i, h_i, p_i) equal to the number of nodes on input layer as that of output layer. For simplicity, we denote the set of environmental data and corresponding data collection rate pair as $\mathcal{X} = \{(t_i, h_i, p_i, z_i)\}$. As the weights ω_{ij} , the center c_m and the width b_m can affect RBFNN, the proper values of these parameters should be determined. In this paper, the RBFNN is trained based on the Gauss-Newton Iterative Cubature Kalman Filter (ICKF). We first give the state X_k as:

$$X_k = [\omega_{11}, \dots, \omega_{mn}, c_1, \dots, c_m, b_1, \dots, b_m],$$

where the number of hidden layer nodes is denoted by m . Then, we have

$$\begin{cases} X_{k+1} = X_k + v_k, \\ Z_k = g(X_k, \mathcal{X}) + u_k \end{cases} \quad (7)$$

where X_k and Z_k are state vector and measurement vector, respectively; u_k and v_k represent the measurement noise and the process noise of mean 0 and covariance R_k and Q_k , respectively; the nonlinear mapping between input and output layer is denoted by $g(\cdot)$ denotes, i.e., $g(X_k, \mathcal{X}) = [g_1, \dots, g_n]^T = W_k \varphi_k$ with

$$W_k = \begin{bmatrix} w_{11} & \cdots & w_{m1} \\ w_{12} & \cdots & w_{m2} \\ \vdots & \vdots & \vdots \\ w_{1l} & \cdots & w_{ml} \end{bmatrix},$$

$$\varphi_k = \begin{bmatrix} \varphi(\mathcal{X}, c_1, b_1) \\ \varphi(\mathcal{X}, c_2, b_2) \\ \vdots \\ \varphi(\mathcal{X}, c_m, b_m) \end{bmatrix}.$$

The details of training process are given as follows:

1. *Time Update*: Evaluate cubature points

$$X_{j,k-1} = S_{k-1} \xi_j + \hat{X}_{k-1},$$

where $chol(\cdot)$ represents Cholesky decomposition and $\{\xi_j\}$ denotes standard volume point set. We obtain the estimated value by substituting the volume point as

$$X_{j,k}^* = f(X_{j,k-1}).$$

Then, state \bar{X} and variance \bar{P}_k are calculated as

$$\bar{X}_k = \sum_{j=1}^m \phi_j X_{j,k}^*,$$

$$\bar{P}_k = \sum_{j=1}^m \phi_j X_{j,k}^* X_{j,k}^{*T} - \bar{X}_k \bar{X}_k^T + Q_{k-1}.$$

where $\phi_i = \frac{1}{2m(n+2)}$.

2. *Measure Update*: The measurement update begins with \bar{X}_k and \bar{P}_k and it is iterated until the stop condition is met. Let the state and the variance estimated in the i th iteration be denoted by $\hat{X}_k^{(i)}$ and $P_k^{(i)}$, respectively. We determine volume points by

$$\begin{aligned} \hat{S}_k^{(i)} &= chol(P_k^{(i)}), \\ X_{j,k}^{(i)} &= \hat{S}_k^{(i)} \xi_j + \hat{X}_k^{(i)}. \end{aligned}$$

The state and variance in the i th iteration are estimated as

$$\begin{aligned} \hat{X}_k^{(i+1)} &= \bar{X}_k + W_k^{(i)} [Z_k - g(\hat{X}_k^{(i)}, \mathcal{X}) \\ &\quad - (P_{xz,k}^{(i)})^T \bar{P}_k^{-1} (\bar{X}_k - \hat{X}_k^{(i)})], \\ P_k^{(i+1)} &= \bar{P}_k - W_k^{(i)} P_{zz,k}^{(i)} (W_k^{(i)})^T, \end{aligned}$$

where $W_k^{(i)} = P_{xz,k}^{(i)} (P_{zz,k}^{(i)})^{-1}$. To reduce the linearized error introduced by truncating high-order terms of taylor expansion, $P_{zz,k}^{(i)}$ and $P_{xz,k}^{(i)}$ are calculated as

$$\begin{aligned} P_{zz,k}^{(i)} &= \sum_{j=1}^m \phi_j Z_{j,k}^{(i)} (Z_{j,k}^{(i)})^T - \hat{Z}_k^{(i)} (\hat{Z}_k^{(i)})^T + R_k, \\ P_{xz,k}^{(i)} &= \sum_{j=1}^m \phi_j X_{j,k}^{(i)} (Z_{j,k}^{(i)})^T - \hat{X}_k^{(i)} (\hat{Z}_k^{(i)})^T, \end{aligned}$$

where $Z_{j,k}^{(i)} = g(X_{j,k}^{(i)}, \mathcal{X})$ and $\hat{Z}_k^{(i)} = \sum_{j=1}^m \phi_j \hat{Z}_{j,k}^{(i)}$. The stop condition is given by

$$\|X_k^{(i+1)} - X_k^{(i)}\| \leq \varepsilon \quad \text{or } i = N_{max},$$

where ε and N_{max} are the predetermined threshold and the maximum iteration number respectively.

Once the training finished in N rounds, the estimated state vector is obtained as $\hat{X}_k = \hat{X}_k^{(N)}$ with $P_k = P_k^{(N)}$. Thus, Dcr_{n_i} can be predicted utilizing (7).

B. ENERGY EFFICIENT TASK DISTRIBUTION

Recall that all data of a component G_i will be collected while a CNIB reached the position p_i^c . That suggests the set $P = \{p_i^c\}$ of data collection positions should be partitioned into N_m nonoverlapping clusters C_i s, each of which is assigned a CNIB responsible to collect and aggregate data for corresponding G_i s. Otherwise, a component, say G_i , could be visited by several CNIBs such that data is lost due to the limited buffer size of each node. That suggests the time gap should have the following constrain

$$\frac{L}{V} \leq \frac{BUF_{n_i}}{DCR_{G_i}} (1 + \eta), \quad (8)$$

where L represents the length of the route, η is the tolerable data loss ratio adapted w.r.t realistic scenarios, and Dcr_{G_i} denotes the data collection rate of component G_i , i.e., $Dcr_{G_i} = \max_{n_i \in G_i} Dcr_{n_i}$. Accordingly, a greedy partitioning algorithm is developed as follows:

Step 1, construct a Hamilton cycle H_P over set P and label each $p_i^c \in H_P$ sequentially along the H_P , i.e., $H_P = p_1^c p_2^c \dots p_n^c p_1^c$, then repeat Step 2 with a different starting position $p_i^c \in H_P$ each time;

Step 2, sequentially add p_i^c to C_j , i.e., $C_j = C_j \cup \{p_i^c\}$, only if $L_{H_{C_j}}$ satisfies (8); Otherwise, add current position p_k^c to C_{j+1} and repeat this step until each $p_i^c \in H_P$ belongs to a certain cluster;

Theorem 1: The Aggregation Ratio of IDAS AR_{IDAS} equals to $\frac{1}{1+\eta}$, only if the tolerable data loss rate η is chosen as

$$\eta = \frac{L(H_{G_i}) * DCR_{n_i}}{V * Buf_{n_i}} - 1. \quad (9)$$

Proof: Let the optimal partition is denoted by G . For each sub-partition $G_i \in G$, we have optimal Hamilton cycle H_{G_i} such that

$$\frac{L(H_{G_i})}{V} \leq \frac{BUF_{n_i}}{DCR_{n_i}},$$

then no data will be lost. That implies $AR_{IDAS} = 100\%$. If $\eta = \max_{G_i \in G} \{\frac{L(H_{G_i}) * DCR_{n_i}}{V * BUF_{n_i}} - 1\}$, then according to (8) we have

$$\frac{L(H_{G_i})}{V} \leq \frac{BUF_{n_i}}{DCR_{n_i}} (1 + \eta).$$

That implies $AR_{IDAS} = \frac{1}{1+\eta}$.

On the other hand, if the tolerable data loss rate is chosen as $\eta' > \eta$, then we have $\frac{L(H_{G_i})}{V} < \frac{BUF_{n_i}}{DCR_{n_i}} (1 + \eta')$. Thus, let a node n_i aggregates $(1 + \eta' BUF_{n_i})$ data, then only $\frac{1}{1+\eta}$ data successfully delivered to the sink. In addition, it can be deduced that $\frac{L(H_{G_i})}{V} > \frac{BUF_{n_i}}{DCR_{n_i}} (1 + \eta')$ only if $\eta' < \eta$.

That suggests the fact of $\frac{L(H_{G'_i})}{V} \leq \frac{BUF_{n_i}}{DCR_{n_i}} (1 + \eta')$ for each $G_i \in G$ only if a subset $G'_i \subset G_i$. Thus, we add each $n_i \in (G_i - G'_i)$ to a G'_i randomly to create G''_i with $\sum |G''_i| = n$. It is obviously that

$$\frac{L(G''_i)}{L(L(H_{G_i}))} \leq 2.$$

Accordingly, we have

$$\begin{aligned} \frac{1}{\frac{8}{3}(1 + \eta)} &= \frac{BUF_{n_i} V}{2DCR_{n_i} 2L(H_{G_i})} \\ &< AR_{IDAS} \\ &< \frac{BUF_{n_i} V}{DCR_{n_i} 2L(H_{G_i})} = \frac{1}{2(1 + \eta)}. \end{aligned}$$

Therefore, the theorem holds. \blacksquare

C. DRL BASED ROUTE DESIGN

We consider the CNIB route design in a continuous multi-agent data aggregation environment. That suggests traditional DRL methods, i.e., DQN, can not be applied to CNIB route design. Therefore, we utilize Deep Deterministic Policy Gradient (DDPG) to design CNIB route. Note that each CNIB m has a state s_t^m at each timeslot t , and is then given an action a_t^m to obtain a reward r_t^m and observe new state s_{t+1}^m from the environment. Before applying DDPG to CNIB route design, we give the definitions of state, action and reward, respectively.

- 1) *State Space:* State is denoted as $S = \{(S_1, S_2, S_3)\}$, in which S_1 represents a cluster C^m of collection positions assigned to a specific CNIB m such that $S_1 = \{(x_t^{k,m}, y_t^{k,m})\}_{k=1}^{|C^m|}$; $S_2 = \{(x_t^m, y_t^m)\}$, where x_t^m, y_t^m are coordinates of CNIB m at timeslot t ; and $S_3 = \{n_t^m\}$ is the number of remaining collection positions m at timeslot t with $n_{t+1}^m = n_t^m - 1$ if a collection position is visited and the corresponding data is collected at next timeslot.
- 2) *Action Space:* Distance d_t^m and moving direction ψ_t^m consists of the action set $A = \{(\psi_t^m, d_t^m) | \psi_t^m \in [0, 2\pi], d_t^m \in [0, d_{max}]\}$.
- 3) *Reward:* Data b_t^m collected by timeslot t , proportion of remaining collection position $n_t^m / |C^m|$, and energy cost \mathbb{E}_T is utilized to calculate reward as:

$$r_t^m = \begin{cases} \frac{1}{\mathbb{E}_T}, & \text{if } b_t^m = 0 \\ \frac{n_t^m b_t^m}{|C^m| \mathbb{E}_T}, & \text{if } b_t^m > 0, \end{cases}$$

Thus, the overall reward is $r_t = \sum_m r_t^m$.

Note that four DNNs are utilized to control each CNIB, i.e., actor network $\pi(s_t|\delta^\pi)$, critic network $Q(s_t, a_t|\eta^Q)$ with randomly initialized weights δ^π, η^Q and target networks with $\delta^{\pi'} = \delta^\pi$ and $\eta^{Q'} = \eta^Q$, where $a_t = (a_t^1, \dots, a_t^{N_m})$ and $s_t = (s_t^1, \dots, s_t^{N_m})$.

For distributed training process, a group of transitions, i.e., $\langle S, A, R \rangle$, is sampled as mini-batches from each CNIB's private buffer. Then, we update critic network Q by minimizing the following function

$$\begin{aligned}\mathcal{L}(\eta^Q) &= E[(\mathcal{Y}_i - Q(s_i, a_i|\eta^Q))^2], \\ \mathcal{Y}_i &= \gamma Q'(s_{i+1}, a_{i+1}|\eta^{Q'}) + r_i,\end{aligned}$$

where $a_i = (a_i^1, \dots, a_i^{N_m})$ and $a_{i+1} = \pi'(s_{i+1})$. Then, the actor network π is updated by

$$\nabla_{\delta^\pi} J = E[\nabla_{\delta^\pi} \pi(s_i|\delta^\pi) \nabla_a Q(s_i, a_i|\eta^Q) | a_i = \pi(s_i)],$$

where $J(\cdot)$ represents the performance function. Target networks are updated w.r.t parameters $\eta^{Q'}$ and $\delta^{\pi'}$ based on a factor ϱ as

$$\begin{aligned}\eta^{Q'} &= \varrho \eta^Q + (1 - \varrho) \eta^{Q'}, \\ \delta^{\pi'} &= \varrho \delta^\pi + (1 - \varrho) \delta^{\pi'}.\end{aligned}$$

D. FERMAT TREE BASED CONNECTION

The last step for restoring data aggregation is to establish inter-cluster connections, for which SNIBs are deployed. As only a limited number of SNIBs are available, N_m closest positions p_i^q 's, each of which locates on the boundary of a specific cluster C_i , are chosen for SNIB deployment along the corresponding Fermat tree. For clarity, we let $T_i^k, f_{T_i}^k$ and $F_{T_i}^k$ denote the triangle, the Fermat point and the corresponding tree built on the k th iteration. Then, the details of Fermat tree construction are given as follows.

Step 1, the Delaunay Triangulation is applied to network G such that the triangulated graph $D_G = \cup T_i$ is established;

Step 2, let each T_i join the set T by such order, only if $T_i \cap T_j = \emptyset, \forall T_j \in T$.

Step 3, at k th iteration, build $F_{T_i}^k$ that consists of two longest edges $e_i, e_j \in F_{T_i}^{k-1}$ and $f_{T_i}^{k-1}$ and repeat this step with $k = k + 1$;

Step 4, after k rounds iterations, we have $F_{T_i} = \cup F_{T_i}^k$;

Step 5, construct a Fermat tree (F) w.r.t the minimum spanning tree (MST) of graph G , i.e., $F = F_{T_1} \cup F_{T_2} \dots \cup MST$, and break cycles if necessary.

Theorem 2: The approximation ratio of SNIB deployment is $\frac{3\sqrt{3}}{4-\sqrt{3}}$.

Proof: In general, a number of triangles t_i 's are discovered based on Delaunay Triangulation. Within each triangle T_i , two longest edges adjacent to the Fermat point $f_{T_i}^k$ is utilized to build a Fermat tree $F_{T_i}^k$ at k th iteration. Note that the length of a Fermat tree is about $\frac{\sqrt{3}}{2}$ times that

of the corresponding MST. Then by induction, it is clear that

$$\begin{aligned}L(F_{T_i}) &\leq \alpha\beta(1 + \alpha\beta + \alpha^2\beta^2 + \dots + \alpha^k\beta^{k-1})L(MST_{T_i}) \\ &< \frac{\alpha\beta}{1 - \alpha\beta}L(MST_{T_i}) \\ &= \frac{\sqrt{3}}{4 - \sqrt{3}}L(MST_{T_i}),\end{aligned}$$

with $\alpha = \frac{\sqrt{3}}{2}$ and $\beta = \frac{1}{2}$. The number of SNIB utilized to connect MST_{T_i} , denoted by $N_{MST_{T_i}}$, is given as $N_{MST_{T_i}} = \frac{L(MST_{T_i}) - 4R}{R}$ [20]. Accordingly, we obtain

$$N_{F_{T_i}} = \frac{L(F_{T_i}) - 2R(k-1) - 6R}{R} + k.$$

It can be deduced that

$$\sum_{T_i} N_{F_{T_i}} \leq \frac{\sqrt{3}}{4 - \sqrt{3}}N_{MST}$$

due to $N_{MST} \geq \sum_{T_i} N_{MST_{T_i}}$. Placing SNIBs along the MST is a 3-approximation algorithm, therefore the approximation ratio of proposed method is $\frac{3\sqrt{3}}{4-\sqrt{3}}$. ■

IV. PERFORMANCE EVALUATION

A. SIMULATION SETUP

The validation experiment of IDAS is conducted on an Intel Core i7-8550u 1.8 GHZ CPU, 16GB RAM computer in Python. In the simulation, we assume that all devices are deployed within $5000m \times 5000m$ area of random terrains. Table 2 gives parameters of this experiment.

TABLE 2. Simulation setup.

Parameter	Description	Value
R	communication radius of NIB	[1000, 1500] m
V	CNIB speed	[20, 90] km/h
N_m	number of CNIB	[4,11]
κ	constant coefficient	10^{-4} j/m ²
ν	energy coefficient	30 j/m
r_c	terrain risk	[0.002,1]
e_c	terrain elevation	[0.5] m

IDAS is first compared with DQNMDC [15], LEEF [2], DRLDC [13], and CISIL [1] in aggregation ratio and energy cost. And the SNIB consumption comparison is conducted between IDAS and baselines OACRQST [21], CRPA [23] and OASS [20].

B. AGGREGATION RATIO

Fig. 1(a) shows the impact of velocity V on aggregation ratio. It is clearly that as V grows the aggregation ratio increases rapidly at first and get stable eventually for each strategy. IDAS outperforms baselines approaches with the highest aggregation ratio. This is because the DRL based energy efficient CNIB route design helps to discover the optimal route such that the trade-off between aggregation ratio and energy cost is achieved.

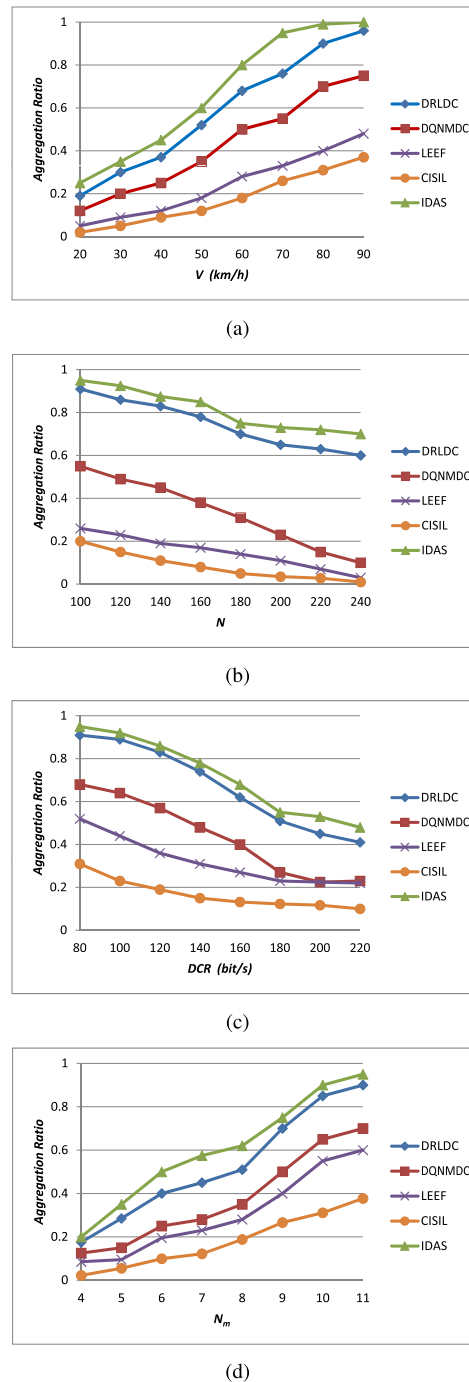


FIGURE 1. Aggregation ratio considering different (a) V , (b) N , (c) Dcr , and (d) N_m .

Observed from Fig. 1(b), we know that as the number of nodes N increases the aggregation ratio decreases for each strategy. The rationale behind that is as follows. More nodes deployed result in longer travelling distance such that there are insufficient time to collect data. However, the travelling distance will increase slowly with a dense population of nodes at last. No doubt that IDAS has the highest aggregation ratio among all strategies.

As shown in Fig. 1(c), the aggregation ratio decreases as data collection rate Dcr increases. In fact, Eq. (8) determines

the relation between the Dcr and the aggregation ratio. That suggests the aggregation ratio will decrease rapidly if the Dcr chosen much larger than a pre-determined threshold. Observed from Fig. 1(c), we know that the highest aggregation ratio is achieved for each strategy if $Dcr = 80\text{bit/s}$ while the lowest aggregation ratio is discovered if $Dcr = 220\text{bit/s}$. IDAS beats all baseline approaches.

The aggregation ratio increases as the growth of the number of CNIBs N_m and eventually stabilise for every strategy (see Fig. 1(d)). The rationale behind that is as follow. With more CNIBs deployed, more data will be collected. Note that the experiment area is fixed such that if the aggregation ratio has approached 100% then no more N_m is needed. IDAS obtains the aggregation ratio much higher than that of baseline approaches.

Fig. 1 suggests the proposed IDAS is more suitable in after disaster scenarios for better data aggregation.

C. ENERGY COST

As shown in Fig. 2(a), the energy cost grows with N . It is clearly that IDAS outperforms all baseline approaches. This is because the DRL based route design helps to reduce the energy cost even if more nodes involved. As shown in Fig. 2(b), as N_m increases the maximum energy decreases. The proposed strategy IDAS performs better than others in a relatively lower maximum energy cost. Besides, N_m seems to affect IDAS less than other strategies due to the consideration of the trade-off between aggregation ratio and energy cost. Both Fig. 2(a) and (b) verify the advantage of the proposed IDAS in energy cost for after disaster scenarios.

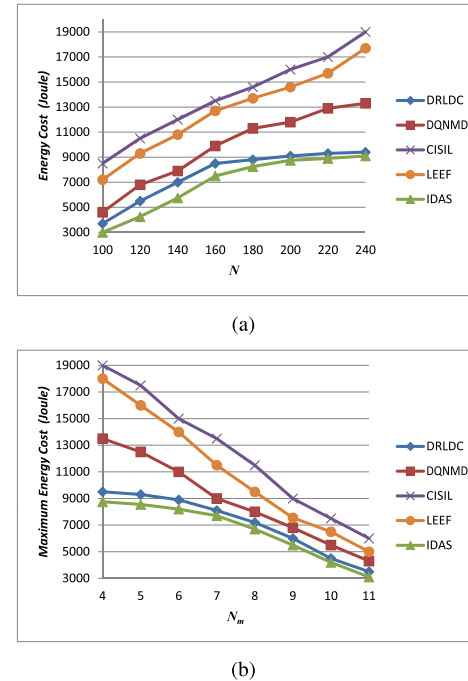


FIGURE 2. The energy cost comparison while varying (a) N and (b) N_m .

D. SNIB CONSUMPTION

As shown in Fig. 3(a), it is evident that SNIBs required for each approach decrease as R increases. The proposed IDAS consumes the least number of SNIBs. This is because IDAS iteratively applies Fermat points to shorten the length of connections between nodes. Observed from Fig. 3(b), we know that as N increases the SNIBs count grows. However, when $N = 180$, the SNIB count drops for all approaches. The rationale behind that is less inter-cluster distances are resulted from a dense population of nodes. The proposed IDAS outperforms all baseline approaches. That indicates the IDAS should be applied to after disaster recovery.

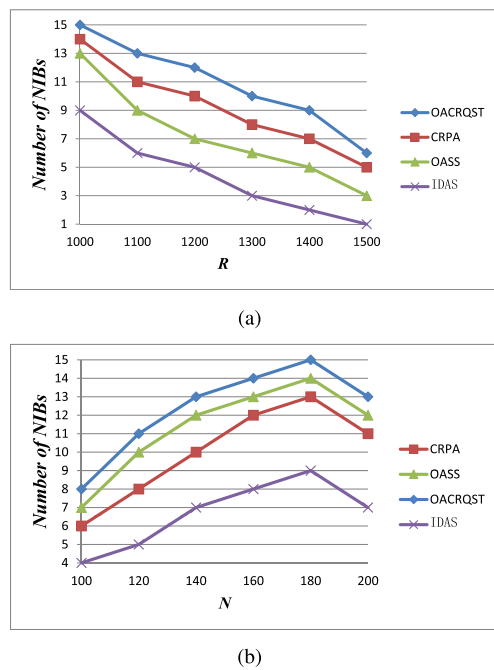


FIGURE 3. The number of SNIB required while varying (a) R and (b) N .

V. CONCLUSION

6G empowered Industrial Internet-of-Everything (IIoE) promises a high quality of services with the consideration of disaster recovery. In this paper, an Intelligent NIB based Data Aggregation Strategy, named (IDAS), is proposed for after disaster scenarios in IIoE. Specifically, IDAS first applies an ICKF-RBFNN to predict the data collection rates of survived infrastructures. Then, an energy efficient task distribution mechanism is developed for the trade-off between the aggregation ratio and the energy cost. Next, a deep reinforcement learning method is employed for car-carrying NIB route design to perform corresponding data collection task. Eventually, all data are aggregated toward the rescue headquarter by NIB deployment based on Fermat tree constructions. The theoretical analysis and simulations indicate that IDAS is not only highly energy efficient for after disaster scenarios but requires the least NIB consumption while compared with contemporary strategies.

REFERENCES

- [1] W. Lalouani, M. Younis, and N. Badache, "Interconnecting isolated network segments through intermittent links," *J. Netw. Comput. Appl.*, vol. 108, pp. 53–63, Apr. 2018.
- [2] S. Lee, M. Younis, B. Anglin, and M. Lee, "LEEF: Latency and energy efficient federation of disjoint wireless sensor segments," *Ad Hoc Netw.*, vol. 71, pp. 88–103, Mar. 2018.
- [3] Y. K. Joshi and M. Younis, "Restoring connectivity in a resource constrained WSN," *J. Netw. Comput. Appl.*, vol. 66, pp. 151–165, May 2016.
- [4] L. Goratti, T. Baykas, T. Rasheed, and S. Kato, "NACRP: A connectivity protocol for star topology wireless sensor networks," *IEEE Wireless Commun. Lett.*, vol. 5, no. 2, pp. 120–123, Apr. 2016.
- [5] Z. Xu, L. Chen, C. Chen, and X. Guan, "Joint clustering and routing design for reliable and efficient data collection in large-scale wireless sensor networks," *IEEE Internet Things J.*, vol. 3, no. 4, pp. 520–532, Aug. 2016.
- [6] A. Abbas and M. Younis, "Establishing connectivity among disjoint terminals using a mix of stationary and mobile relays," *Comput. Commun.*, vol. 36, no. 13, pp. 1411–1421, Jul. 2013.
- [7] X. Wang, L. Xu, S. Zhou, and W. Wu, "Hybrid recovery strategy based on random terrain in wireless sensor networks," *Sci. Program.*, vol. 2017, pp. 1–19, Jan. 2017.
- [8] I. F. Senturk, K. Akkaya, and S. Jananefat, "Towards realistic connectivity restoration in partitioned mobile sensor networks," *Int. J. Commun. Syst.*, vol. 29, no. 2, pp. 230–250, Jan. 2016.
- [9] G. Robins and A. Zelikovsky, "Tighter bounds for graph Steiner tree approximation," *SIAM J. Discrete Math.*, vol. 19, no. 1, pp. 122–134, Jan. 2005.
- [10] D. Chen, D.-Z. Du, X.-D. Hu, G.-H. Lin, L. Wang, and G. Xue, "Approximations for Steiner trees with minimum number of Steiner points," *J. Global Optim.*, vol. 18, no. 1, pp. 17–33, 2000.
- [11] J. Liu, H. Shen, L. Yu, H. S. Narman, J. Zhai, J. O. Hallstrom, and Y. He, "Characterizing data deliverability of greedy routing in wireless sensor networks," *IEEE Trans. Mobile Comput.*, vol. 17, no. 3, pp. 543–559, Mar. 2018.
- [12] W. Zhou, X. Li, J. Yi, and H. He, "A novel UKF-RBF method based on adaptive noise factor for fault diagnosis in pumping unit," *IEEE Trans. Ind. Informat.*, vol. 15, no. 3, pp. 1415–1424, Mar. 2019.
- [13] C. H. Liu, Q. Lin, and S. Wen, "Blockchain-enabled data collection and sharing for industrial IoT with deep reinforcement learning," *IEEE Trans. Ind. Informat.*, vol. 15, no. 6, pp. 3516–3526, Jun. 2019.
- [14] J. Wang, H. Zhang, Z. Ruan, T. Wang, and X. Wang, "A machine learning based connectivity restoration strategy for industrial IoTs," *IEEE Access*, vol. 8, pp. 71136–71145, 2020.
- [15] K. Toyoshima, T. Oda, M. Hirota, K. Katayama, and L. Barolli, "A DQN based mobile actor node control in WSAN: Simulation results of different distributions of events considering three-dimensional environment," in *Proc. Int. Conf. Emerg. Internetworking, Data Web Technol.* Cham, Switzerland: Springer, 2020, pp. 197–209.
- [16] A. Efrat, S. P. Fekete, J. S. B. Mitchell, V. Polishchuk, and J. Suomela, "Improved approximation algorithms for relay placement," *ACM Trans. Algorithms*, vol. 12, no. 2, pp. 1–28, Feb. 2016.
- [17] D. Yang, S. Misra, X. Fang, G. Xue, and J. Zhang, "Two-tiered constrained relay node placement in wireless sensor networks: Computational complexity and efficient approximations," *IEEE Trans. Mobile Comput.*, vol. 11, no. 8, pp. 1399–1411, Aug. 2012.
- [18] S. Misra, S. Don Hong, G. Xue, and J. Tang, "Constrained relay node placement in wireless sensor networks: Formulation and approximations," *IEEE/ACM Trans. Netw.*, vol. 18, no. 2, pp. 434–447, Apr. 2010.
- [19] X. Wang, L. Xu, and S. Zhou, "Restoration strategy based on optimal relay node placement in wireless sensor networks," *Int. J. Distrib. Sensor Netw.*, vol. 11, no. 7, Jul. 2015, Art. no. 409085.
- [20] X. Wang, L. Xu, and S. Zhou, "A straight skeleton based connectivity restoration strategy in the presence of obstacles for WSNs," *Sensors*, vol. 17, no. 10, p. 2299, Oct. 2017.
- [21] B. Chen, H. Chen, and C. Wu, "Obstacle-avoiding connectivity restoration based on quadrilateral Steiner tree in disjoint wireless sensor networks," *IEEE Access*, vol. 7, pp. 124116–124127, 2019.
- [22] A. Uwitonze, J. Huang, Y. Ye, and W. Cheng, "Connectivity restoration in wireless sensor networks via space network coding," *Sensors*, vol. 17, no. 4, p. 902, Apr. 2017.
- [23] R. Kumar and T. Amgoth, "Adaptive cluster-based relay-node placement for disjoint wireless sensor networks," *Wireless Netw.*, vol. 26, no. 1, pp. 651–666, Jan. 2020.

- [24] M. Pozza, A. Rao, H. Flinck, and S. Tarkoma, "Network-in-a-box: A survey about on-demand flexible networks," *IEEE Commun. Surveys Tuts.*, vol. 20, no. 3, pp. 2407–2428, 3rd Quart., 2018.
- [25] M. M. Sohul, M. Yao, X. Ma, E. Y. Imana, V. Marojevic, and J. H. Reed, "Next generation public safety networks: A spectrum sharing approach," *IEEE Commun. Mag.*, vol. 54, no. 3, pp. 30–36, Mar. 2016.



MIN PENG received the bachelor's degree in computer science from the Lanzhou University of Technology, China, in 2018. He is currently pursuing the master's degree with the School of Mathematics and Information, Fujian Normal University. His research interests include blockchain, deep learning, and network security.



ABBAS BRADAI (Member, IEEE) received the Ph.D. degree from the University of Bordeaux, France, in 2012. He is currently working as an Associate Professor at the University of Poitiers, where he has also been a member of the XLIM Research Institute (CNRS UMR 7252), since September 2015. His research interests include multimedia communications over wired and wireless networks, the IoT, software-defined network, and virtualization. He is/was involved in many French and European projects (FP7 and H2020), such as ENVISION and VITAL.



HUI LIN received the Ph.D. degree in computing system architecture from the College of Computer Science, Xidian University, China, in 2013. He is currently a Professor at the College of Mathematics and Informatics, Fujian Normal University, Fuzhou, China, where he is also a M.E. Supervisor with College of Mathematics and Informatics. His research interests include mobile cloud computing systems, blockchain, and network security. He has published more than 50 papers in international journals and conferences.



SAHIL GARG (Member, IEEE) is currently working as a Postdoctoral Research Fellow with the Department of Electrical Engineering, École de technologie supérieure, Université du Québec, Montreal, Canada. His research interests include machine learning, big data analytics, knowledge discovery, cloud computing, the Internet of Things, software-defined networking, and vehicular ad-hoc networks. Some of his research findings are published in top-tier journals and various international conferences. He is a member of ACM. He was a recipient of the prestigious Visvesvaraya Ph.D. Fellowship from the Ministry of Electronics & Information Technology under the Government of India, from 2016 to 2018. For his research, he also received the IEEE ICC Best Paper Award at Kansas City, USA, in 2018. He serves/served as the Workshop Chair Publicity Co-Chair for several IEEE/ACM conferences, including the IEEE INFOCOM, the IEEE GLOBECOM, the IEEE ICC, and ACM MobiCom. In addition, he also serves as the Workshops and Symposia Officer of the IEEE ComSoc Emerging Technology Initiative on Aerial Communications. He serves as the Managing Editor of *Human-centric Computing and Information Sciences (HCIS)* journal (Springer). He is also an Associate Editor of the *IEEE Network Magazine*, Future Generation Computer Systems (FGCS) (Elsevier), and International Journal of Communication Systems (IJCS) (Wiley). He has guest edited a number of special issues in top-cited journals, including the IEEE TRANSACTIONS ON INTELLIGENT TRANSPORTATION SYSTEMS, the IEEE TRANSACTIONS ON INDUSTRIAL INFORMATICS, the IEEE INTERNET OF THINGS JOURNAL, the IEEE Network Magazine, and Future Generation Computer Systems (Elsevier).



XIAODING WANG received the Ph.D. degree from the College of Mathematics and Informatics, Fujian Normal University, in 2016. He is an Associate Professor with the School of Fujian Normal University, China. His main research interests include network optimization and fault tolerance.

M. SHAMIM HOSSAIN (Senior Member, IEEE) received the Ph.D. degree in electrical and computer engineering from the University of Ottawa, Canada, in 2019. He is currently a Professor at the Department of Software Engineering, College of Computer and Information Sciences, King Saud University, Riyadh, Saudi Arabia. He is also an Adjunct Professor at the School of Electrical Engineering and Computer Science, University of Ottawa, Canada. His research interests include cloud networking, smart environment (smart city and smart health), AI, deep learning, edge computing, the Internet of Things (IoT), multimedia for health care, and multimedia big data. He has authored and coauthored more than 260 publications, including refereed journals conference papers, books, and book chapters. Recently, he co-edited a book on "Connected Health in Smart Cities," (Springer). He is a Senior Member of ACM. He was a recipient of the number of awards, including the Best Conference Paper Award at the 2016 ACM Transactions on Multimedia Computing, Communications and Applications (TOMM) Nicolas D. Georganas Best Paper Award, and the 2019 King Saud University Scientific Excellence Award (Research Quality). He has served as the co-chair, the general chair, the workshop chair, the publication chair, and TPC for more than 12 IEEE and ACM conferences and workshops. He is currently the Co-Chair of the 3rd IEEE ICME workshop on Multimedia Services and Tools for Smart-Health (MUST-SH 2020). He is on the Editorial Board of the IEEE TRANSACTIONS ON MULTIMEDIA, the IEEE MULTIMEDIA, the IEEE NETWORK, the IEEE WIRELESS COMMUNICATIONS, IEEE ACCESS, *Journal of Network and Computer Applications* (Elsevier), and *International Journal of Multimedia Tools and Applications* (Springer). He serves/served as a Guest Editor of the *IEEE Communications Magazine*, the IEEE NETWORK, the IEEE TRANSACTIONS ON INFORMATION TECHNOLOGY IN BIOMEDICINE (currently JBHI), and the IEEE TRANSACTIONS ON CLOUD COMPUTING. He also serves as a Lead Guest Editor of *ACM Transactions on Internet Technology*, *ACM Transactions on Multimedia Computing, Communications, and Applications* (TOMM), *Multimedia Systems* journal, *International Journal of Multimedia Tools and Applications* (Springer), *Cluster Computing* (Springer), *Future Generation Computer Systems* (Elsevier), *Computers and Electrical Engineering* (Elsevier), *Sensors* (MDPI), and *International Journal of Distributed Sensor Networks*.